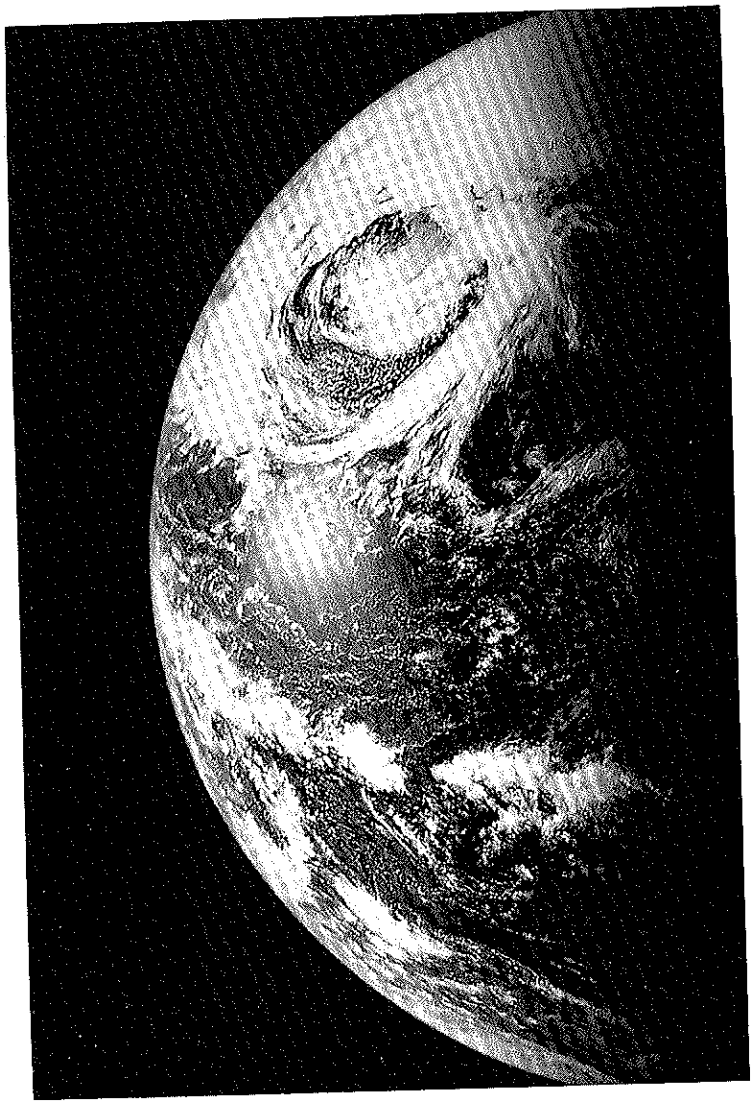

Photograph taken by astronauts aboard the *Apollo Saturn* spacecraft during April 1970. The picture is centered over the north Pacific Ocean. The Kamchatka Peninsula of Siberia can be seen just northwest of a large oceanic extratropical cyclone. The sun's reflection off the ocean surface is seen to the south of the storm. A belt of mesoscale convective cloud systems extends east–west near the equator.

This is Volume 53 in the
INTERNATIONAL GEOPHYSICS SERIES
A series of monographs and textbooks
Edited by RENATA DMOWSKA and JAMES R. HOLTON

A complete list of the books in this series appears at the end of this volume.

Cloud Dynamics

Robert A. Houze, Jr.
DEPARTMENT OF ATMOSPHERIC SCIENCES
UNIVERSITY OF WASHINGTON
SEATTLE, WASHINGTON

ACADEMIC PRESS, INC.
A Division of Harcourt Brace & Company
San Diego New York Boston
London Sydney Tokyo Toronto

trajectory over the water. One result is the formation of an *arctic front* at the leading edge of the air that originated recently over the ice.

In this situation, there are several factors that can affect the dynamical evolution of the polar low. In particular: (i) A feature like the arctic front is always susceptible to cyclogenetic stimulation by the passage of an upper-level trough (as in Fig. 11.5). (ii) As we saw in Chapter 10, the tropical cyclone draws its energy almost wholly from the ocean surface as boundary-layer mixing is stimulated by strong winds over the warmer water. In the polar low, there is also a considerable disequilibrium at the sea surface, in this case because of the large temperature contrast between air and ocean. Thus, hurricane-like dynamics are feasible. (iii) The polar low forms in an environment where the vertical thermal stratification exhibits considerable buoyant instability (Sec. 2.9.1). As a result, some of the energy of the storm may be drawn from convective available potential energy (CAPE, Sec. 8.4) stored in the vertical temperature gradient. Any or all of these energy sources may be tapped in a given case of polar-low development. Given the multiplicity of viable energy sources, it is understandable that a variety of observed polar-low structures exist. The cases exhibiting hurricane-like cloud structure may be those that depend to a significant extent on (ii). However, this topic remains one of active research.

Chapter 12 | Orographic Clouds

"...towering up the darkening mountain's side...
It mantles round the mid-way height..."[320]

In previous chapters, we have seen a variety of dynamical features that govern the air motions in clouds. These include turbulence and entrainment in layer clouds, buoyancy, pressure perturbation, entrainment, and vorticity in cumulus and cumulonimbus, mesoscale circulations in complexes of thunderstorms, and secondary circulations associated with the winds and thermal patterns of hurricanes, baroclinic waves, and fronts. There remains one important source of air motions in clouds that we have not yet discussed: the flow of air over hills and mountains. In this chapter, we consider this subject by examining the dynamics of cloud-producing air motions induced by wind blowing over terrain.

It is evident that when a fluid on the earth is flowing over an uneven, solid lower boundary, the vertical velocity of the fluid at the interface will be upward or downward, depending on the horizontal direction of the fluid flow relative to the slope of the bottom topography. Since the fluid is a continuous medium, the vertical motion at the bottom will be felt through some depth extending above the lower boundary. Clouds can form if the air forced over the terrain is sufficiently moist. Moreover, since restoring forces exist in the fluid, the vertical motion produced there by the lower boundary can excite waves. Thus, the vertical motion produced in a fluid by flow over terrain can include alternating regions of upward and downward motion, which may extend above, downstream, or upstream of the hill. Clouds can form in the upward-motion areas of the waves. Nonprecipitating clouds that form in moist layers in direct response to the wave motions induced by flow over topography are referred to as wave clouds. These clouds often take the form of lenticular clouds (Figs. 1.18–1.22) and rotor clouds (Figs. 1.23 and 1.24), which are visually spectacular tracers of the atmospheric wave motions in mountainous regions. Precipitating clouds can also be formed or modified by the flow over orography. Stable nimbostratus clouds can be formed or enhanced by upslope motions and dried out by downslope motions, while the formation of cumulonimbus clouds may be triggered in several ways by flow over terrain.

In this chapter, we will first consider clouds that form where air in the boundary layer is forced to flow upslope (Sec. 12.1). Then we will consider the more com-

[320] Goethe's reference to a cloud enveloping the top of a mountain.

plex subject of clouds that form in association with waves excited by flow over varying topography. In Sec. 12.2, we will examine waves and clouds that form in response to flow over two-dimensional mountain ridges. In Sec. 12.3, we will extend the discussion to three dimensions by considering cloud formation produced by flow over isolated mountain peaks. Finally, in Sec. 12.4, we will examine the effect of flow over topography on precipitating clouds.

12.1 Shallow Clouds in Upslope Flow

A simple boundary condition applies in all of our considerations of flow over topography. Since the earth's surface is fixed, the component of air motion normal to the surface must vanish at the ground. The vertical wind component at the surface w_o is then

$$w_o = (\mathbf{v}_H)_o \cdot \nabla \hat{h} \tag{12.1}$$

where $(\mathbf{v}_H)_o$ is the horizontal wind at the surface and $\hat{h}$ is the height of the terrain. It follows that wherever a shallow layer of air is flowing horizontally toward rising terrain, cloud will form near the surface. Air can be directed up a slope for a host of reasons, ranging from purely local effects over a small hill to widespread synoptic-scale flow over gently sloping terrain (such as when low-level easterly flow prevails over the central United States and low clouds cover the entire Great Plains, which slope gradually upward toward the Rocky Mountains). The clouds that form in upslope flow are often in the form of fog or stratus confined to low levels (Fig. 12.1). However, they may be deep enough to produce drizzle or other light precipitation.

12.2 Wave Clouds Produced by Long Ridges[321]

In certain wind and thermodynamic stratifications, the boundary condition (12.1) is felt through a deep layer. As the surface air is forced to move up and down over the topography, restoring forces in the atmosphere come into play and a variety of wave motions can occur. Associated with the waves are substantial vertical motions, which can lead to clouds if the layers of air affected are sufficiently moist. To gain an appreciation of the dynamics of these clouds, we will examine the physics of the various waves excited by wind blowing over irregular terrain. To simplify matters, we restrict the discussion of this section to air flowing over uniform, infinitely long ridges. This case is physically distinct from the flow over three-dimensional hills or mountain peaks. In the case of a ridge, air has no opportunity to flow around the barrier; it must either flow over the ridge or be blocked. In contrast, for an isolated peak in the terrain, air may flow around the

[321] Much of the material in this section is based on review articles by Durran (1986b, 1990) and on Chapter 9 of Holton (1992).

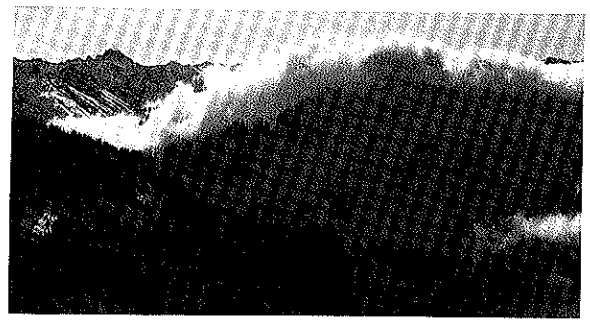

Figure 12.1 Upslope fog. Cascade Mountains, Washington. (Photo by Steven Businger.)

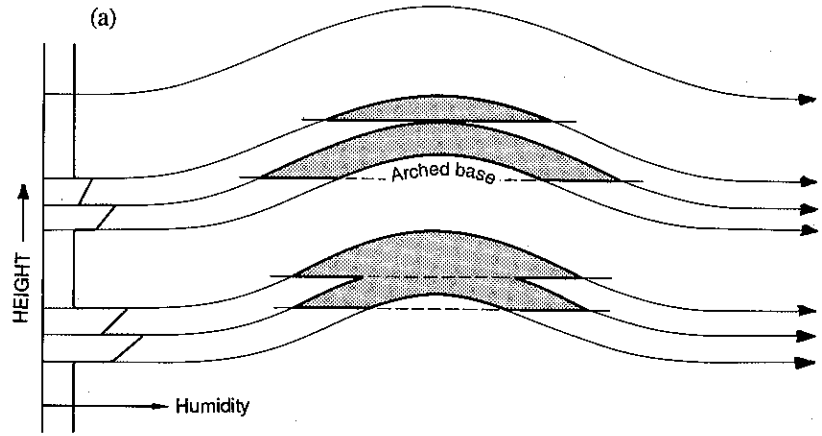

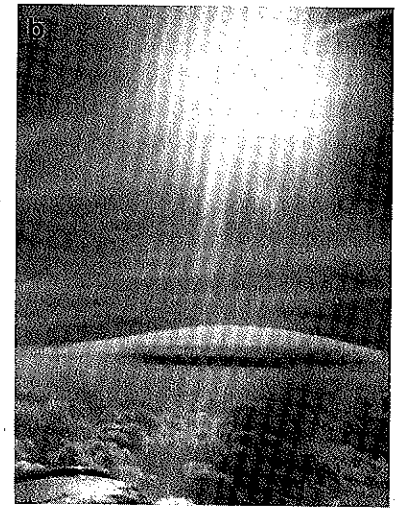

Figure 12.2 Layered structure of wave clouds. (a) Streamlines show airflow. On the left is an imagined profile of relative humidity, each layer with its own condensation level. The corresponding wave-cloud shapes downwind are outlined and shaded. Arched base occurs if the layer of air lifted is dry enough. (b) Photograph of a lenticular cloud downwind of Mt. Rainier, Washington. (Diagram adapted from Scorer, 1972; photo by Arthur L. Rangno.)

obstacle, and thus more possibilities for flow patterns arise. The three-dimensional case will be considered in Sec. 12.3, where we will treat it as an extension of the two-dimensional case.

To simplify the mathematics in both this section and Sec. 12.3, we will consider the air to be unsaturated. The thermodynamic equation thus reduces to the conservation of potential temperature (2.11). Since our primary objective here is to describe the dynamics of clouds, it may appear contradictory to ignore the effects of condensation; however, mathematical strategies exist for taking the condensation into account quantitatively. For example, one can switch to conservation of equivalent potential temperature (2.18) once condensation begins. For our purposes, however, the resulting modifications of the mathematics are unnecessarily complex, since it turns out that the air motions in mountain waves are not qualitatively altered by the occurrence of condensation in the flow. The patterns of cloud formation in the flow over topography can be readily inferred from the vertical air motion calculated ignoring condensation. Wherever a layer of air is subjected to upward motion as a result of the topographically induced wave motions and is sufficiently moist, a cloud will form. This process is illustrated in Fig. 12.2, which indicates how wave perturbations of the flow in the x–z plane can lead to lenticular cloud forms in layers of elevated relative humidity. Note how discontinuities in the humidity layering can lead to an arched cloud base and to stacks of lenticular clouds.

12.2.1 Flow over Sinusoidal Terrain

We first examine the dry-adiabatic flow over a series of sinusoidally shaped two-dimensional ridges of infinite length parallel to the y-axis. Although this is a rather idealized case, it is nonetheless useful. It illustrates the essential physics of the problem, and it is easily extended to the case of a ridge of arbitrary shape, since the latter can be considered a superposition of sinusoidal profiles of different wavelengths.

We have seen in previous chapters that vertical motions in clouds are often revealed through a consideration of the generation and redistribution of horizontal vorticity. This approach is again useful in considering air motions generated by flow over terrain. For two-dimensional Boussinesq flow in the x–z plane, vorticity about the y-axis (ξ) is generated by horizontal gradients of buoyancy, according to (2.61). As the paths of fluid parcels are tipped upward and downward by the surface topography, horizontal gradients of vertical velocity are created in the fluid. According to (2.11), the alternating regions of upward and downward motion, in turn, introduce alternating regions of adiabatic cooling and warming. The alternating cool and warm regions thus generated constitute horizontal gradients of buoyancy, which then generate horizontal vorticity ξ according to (2.61). If the flow over the terrain adjusts to steady state, (2.61) reduces to

$$u\xi_x + w\xi_z = -B_x \tag{12.2}$$

The variables in this equation may be written, as discussed in Sec. 2.6, in terms of perturbations (indicated by a prime) from a mean state (indicated by an overbar). If the perturbations of the flow are of small amplitude, they are described by linearizing (as discussed in Sec. 2.6.2) about a state of mean motion $[\bar{u}(z),\bar{w} = 0]$, where $\bar{u}(z)$ is the mean-state flow in the x-direction (i.e., normal to the ridges in the topography). First linearizing the right-hand side of (12.2) we obtain

$$u\xi_x + w\xi_z = \frac{w}{\bar{u}}\bar{B}_z \tag{12.3}$$

where we have substituted for B_x' from the steady-state version of (2.106). From (12.3), it is evident that the steady-state velocity field must be arranged so that the advection of vorticity just balances the buoyancy generation constituted by the adiabatic cooling and warming associated with the perturbations of vertical motion. Since the fluid is moving horizontally as well as vertically, the temperature perturbations produced by vertical motion w are spread over a horizontal distance by the horizontal velocity component $\bar{u}$, thus determining a horizontal gradient of B, the effect of which must be balanced by the advection.

When the advection terms on the left-hand side of (12.3) are linearized, after making use of the definition $\xi \equiv u_z - w_x$ and invoking the mass continuity equation (2.55), we obtain

$$w_{zz} + w_{xx} + \ell^2 w = 0 \tag{12.4}$$

where ℓ^2 is the *Scorer parameter*, defined as

$$\ell^2 \equiv \frac{\bar{B}_z}{\bar{u}^2} - \frac{\bar{u}_{zz}}{\bar{u}} \tag{12.5}$$

Equation (12.4) is simply the steady-state form of (2.107), whose solutions are internal gravity waves. The patterns of vorticity generated by the flow over topography thus take the form of gravity waves. The general solution of (12.4) when ℓ^2 is a constant is

$$w = \mathrm{Re}\left[\hat{w}_1 e^{i(kx+mz)} + \hat{w}_2 e^{i(kx-mz)}\right] \tag{12.6}$$

where $\hat{w}_1$ and $\hat{w}_2$ are constants and

$$m^2 = \ell^2 - k^2 \tag{12.7}$$

Thus, the vertical structure of the waves depends on the relative magnitude of the Scorer parameter and the horizontal wave number. If $k > \ell$, then the solution (12.6) decays or amplifies exponentially with height. If $k < \ell$, then the wave varies sinusoidally in z with wave number m.

The values of the basic-state wind profile $\bar{u}(z)$ and static stability $\bar{B}_z$ are considered to be those measured upstream of the mountain ridge. If these values are given, then so is ℓ^2 [according to (12.5)]. The field of w is obtained by solving (12.4) under the constraint of appropriate boundary conditions at the earth's sur-

face and as $z \to \infty$. The horizontal velocity field follows readily from $w(x,z)$ by mass continuity since the two-dimensional form of the Boussinesq continuity equation (2.55) is simply

$$u_x + w_z = 0 \tag{12.8}$$

and the upstream horizontal velocity $\bar{u}(z)$ is given.

The lower-boundary condition imposed in solving (12.4) is simply the linearized form of (12.1). If the sinusoidal surface topography is represented mathematically by

$$\hat{h} = h_a \cos kx \tag{12.9}$$

where h_a is a constant and k is an arbitrary wave number, then (12.1) implies that

$$w_o = -\bar{u}_o h_a k \sin kx \tag{12.10}$$

This lower-boundary condition is called *free slip*. The appropriate upper-boundary condition depends on whether the wave solution varies exponentially with height ($k > \ell$) or sinusoidally ($k < \ell$). In either case, the fundamental factor is that the mountains at the lower boundary are the energy source for the disturbance. If $k > \ell$, solutions that amplify exponentially as z increases are regarded as physically unreasonable and set to zero. If $k < \ell$, any waves that transport energy downward are set to zero, while those that transport energy upward are retained; this assumption is called the *radiation boundary condition*. It can be shown that the waves retained by the radiation boundary condition are those whose phase lines tilt upstream as z increases.[322]

Application of these lower- and upper-boundary conditions[323] leads to

$$w(x,z) = \begin{cases} -\bar{u} h_a k e^{-\hat{\mu} z} \sin kx, & k > \ell \\ -\bar{u} h_a k \sin(kx + mz), & k < \ell \end{cases} \tag{12.11}$$

where $\hat{\mu}^2 \equiv -m^2$, and $\hat{\mu}$ is thus a positive number, emphasizing that in the case of $k > \ell$ the waves decay exponentially with height. These waves are referred to as *evanescent* (i.e., fading away). In the case of $k < \ell$ (i.e., for wider mountains), the waves propagate vertically without loss of amplitude. These two types of wave structure are illustrated in Fig. 12.3 for a case of constant $\bar{u}$ and $\bar{B}_z$. It is clear from these examples how the flow stays in phase with the mountains but dies out with height in the narrow-ridge case ($k > \ell$, Fig. 12.3a), while in the wide-ridge case ($k < \ell$, Fig. 12.3b), the waves retain their amplitude with height but have ridge and trough lines sloping upstream.

12.2.2 Flow over a Ridge of Arbitrary Shape

Although the infinite series of sinusoidal ridges considered in the previous subsection are useful to illustrate the two basic types of wave structure that can arise

[322] See Durran (1986b).
[323] *Ibid.*

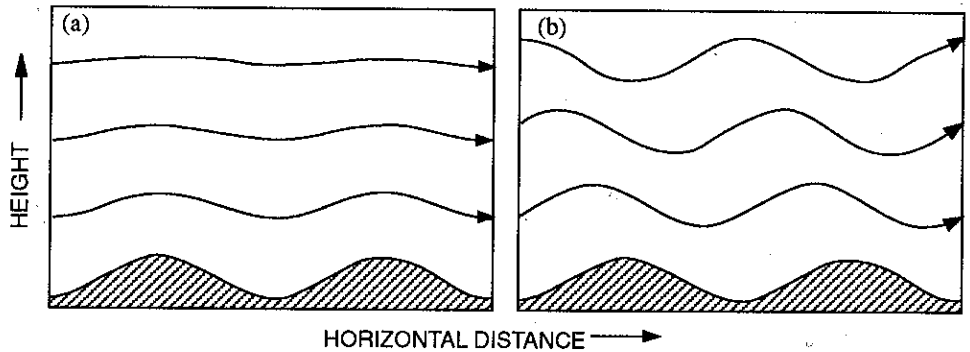

Figure 12.3 Streamlines in the steady airflow over an infinite series of sinusoidal ridges when (a) the wave number of the topography exceeds the Scorer parameter (narrow ridges) or (b) the wave number of the topography is less than the Scorer parameter (wide ridges). Shading indicates bottom topography. (From Durran, 1986b. Reprinted with permission from the American Meteorological Society.)

from airflow across the terrain, they are very special in that they excite only k, the horizontal wave number of the terrain itself. When the topography has any other shape, a spectrum of waves is activated. To see this, consider a single mountain ridge of arbitrary shape $\hat{h}(x)$. This shape can be represented by a Fourier series

$$\hat{h}(x) = \sum_{s=1}^{\infty} \mathrm{Re}\left[h_s e^{ik_s x}\right] \tag{12.12}$$

That is, the terrain profile is the superposition of sinusoidal profiles like (12.9). The solution of (12.4) for each such profile (of wave number k_s) is of the form (12.6). The solution for the arbitrary profile $\hat{h}(x)$ is the sum of all of these solutions for individual wave numbers. After application of the free slip and radiation boundary conditions, the total solution takes the form

$$w(x,z) = \sum_{s=1}^{\infty} \mathrm{Re}\left[i\bar{u}_o k_s h_s e^{i(k_s x + m_s z)}\right] \tag{12.13}$$

The individual Fourier modes contributing to this expression each behave as the total solution for periodic sinusoidal topography. The individual modes will thus be vertically propagating or vertically decaying, depending on whether m_s is real or imaginary (i.e., on whether $k_s > \ell$ or $k_s < \ell$). If the ridge is narrow, wave numbers $k_s > \ell$ dominate the solution and the resulting disturbance is primarily evanescent. If the ridge is wide, wave numbers $k_s < \ell$ dominate, and the disturbance propagates vertically.

A bell-shaped ridge of the form

$$\hat{h}(x) = \frac{h_a a_H^2}{a_H^2 + x^2} \tag{12.14}$$

illustrates the behavior of the solutions summed in (12.13). Since $\hat{h} = h_a$ at $x = 0$ and $\hat{h} = h_a/2$ at $x = \pm a_H$, a_H^{-1} is a scale characteristic of the dominant wave numbers forced by the mountain. The solution for a narrow mountain ($a_H^{-1} \gg \ell$) is illustrated in Fig. 12.4a. The disturbance, dominated by exponentially decaying solutions, is symmetric with respect to the crest of the ridge and decays strongly with height. An example of a wide-mountain solution ($a_H^{-1} \ll \ell$) is shown in Fig. 12.4c. If it is assumed that this case is equivalent to taking $k \ll \ell$, then the solution is hydrostatic and the dominant terms in (12.13) are of the form

$$i\bar{u}_o k_s h_s e^{i(k_s x + \ell z)} \tag{12.15}$$

Thus, the dependence of vertical wavelength on horizontal wavelength disappears, and the mountain profile is reproduced at every altitude that is an integral multiple of $2\pi/\ell$. It can be shown that the horizontal component of the group velocity (Sec. 2.7.2) of a stationary two-dimensional hydrostatic wave is zero. Hence, the energy propagation (which is in the direction of the group velocity) is purely vertical. Thus, for the mountain ridge that is wide enough to excite hydrostatic waves (but not large enough for Coriolis force to be important), the disturbance occurs directly over the ridge, and at any given height there is only one wave crest in the flow.

The intermediate case in which $a_H^{-1} = \ell$ is illustrated in Fig. 12.4b. In this case, the solution (12.13) is dominated by vertically propagating *nonhydrostatic* waves ($k < \ell$ but not $\ll \ell$). The phase lines of these waves still slope upstream, and energy is transported upward. However, unlike hydrostatic waves, the nonhydrostatic waves also have a horizontal component of group velocity (and hence energy propagation) in the downstream direction. As a result, additional wave crests appear aloft downstream of the mountain ridge.

12.2.3 Clouds Associated with Vertically Propagating Waves

We can now see how certain types of wave clouds are produced. If a stratum within the air flowing over the ridge undergoes strong upward displacement as part of a vertically propagating wave (either hydrostatic or nonhydrostatic), clouds will appear. For illustration, possible locations of clouds associated with vertically propagating waves are shaded in Fig. 12.4b and c. Lower-level clouds form upstream of and over the ridge. Upper-level clouds (usually cirrus or cirrostratus) may be found downstream of the ridge. These theoretical cases indicate that the horizontal scale of clouds associated with vertically propagating waves is ~10–50 km. An example of clouds associated with vertically propagating wave motion like that in Fig. 12.4c can be seen in Fig. 12.5. The lower-level cloud over the Continental Divide in the background and the upper-level cirriform cloud in the foreground are associated with the vertically propagating waves' upward air motion, which is found upstream of the crest of the ridge at low levels and downstream of the crest at upper levels.

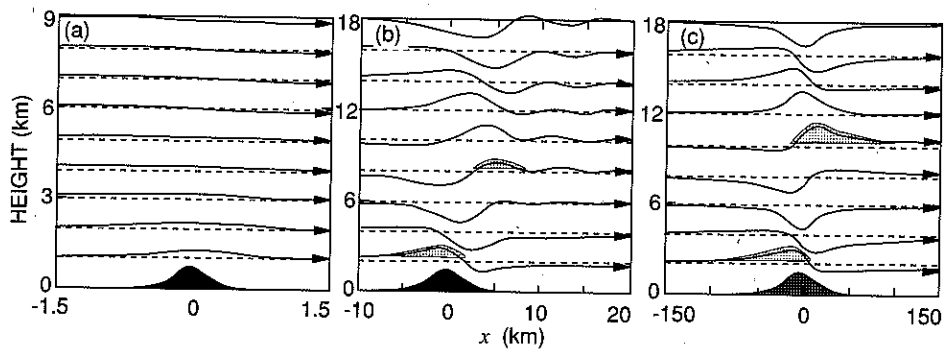

Figure 12.4 Streamlines in the steady airflow over an isolated bell-shaped ridge. (a) Narrow ridge. (b) Width of ridge comparable to the Scorer parameter. (c) Wide ridge. Lighter shading indicates possible locations of clouds. Darker shading indicates bottom topography. (From Durran, 1986b Reprinted with permission from the American Meteorological Society.)

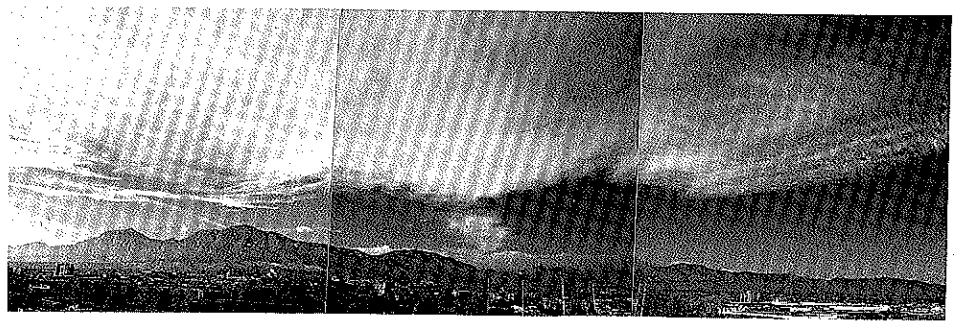

Figure 12.5 Looking upwind at clouds associated with vertically propagating waves. In the center background, a lower-level wave cloud is evident directly over the Continental Divide, which is the main orographic barrier. The mountains in the foreground, which appear larger in the photo, are actually smaller foothills. The cirriform cloud deck at higher levels is produced by the upward air motion associated with the vertically propagating wave induced by the Divide. These clouds are like those indicated schematically in Fig. 12.4c. Boulder, Colorado. (Photo by Dale R. Durran.)

12.2.4 Clouds Associated with Lee Waves

So far we have considered only situations in which ℓ^2 is constant with respect to height. When ℓ^2 decreases suddenly with increasing height, a different type of mountain wave occurs. This type of disturbance is usually called a *lee wave*, but it is also known as a *resonance wave*, *trapped wave*, or *trapped lee wave*. According to (12.5), a decrease of ℓ^2 can be brought on by a decrease of $\bar{B}_z$, an increase of $\bar{u}$, or a change of the curvature of the wind profile $\bar{u}_{zz}$. The occurrence of lee waves can be illustrated by considering a two-level stratification of ℓ^2, in which ℓ_L^2 and ℓ_U^2 represent the Scorer parameters for the lower and upper layers, respectively. Then two equations of the form (12.4) can be applied, one with each value of ℓ^2. Solutions to the upper-layer equation decay exponentially with height, while solu-

tions to the lower-layer equation are sinusoidal in z (i.e., propagate vertically). The solutions are required to match smoothly at the interface, which is taken to be $z = 0$. When the radiation boundary condition is applied, the solution of the upper-layer equation takes the form

$$w_u = \hat{A}e^{-\mu_u z} f(x) \tag{12.16}$$

where $f(x)$ represents the variability in x, and

$$\mu_u \equiv \sqrt{k^2 - \ell_U^2} \tag{12.17}$$

The solution in the lower layer is of the form

$$w_l = \left(\hat{B}\sin m_l z + \hat{C}\cos m_l z\right) f(x) \tag{12.18}$$

where $\hat{B}$ and $\hat{C}$ are constants and

$$m_l \equiv \sqrt{\ell_L^2 - k^2} \tag{12.19}$$

Both (12.16) and (12.18) are special cases of the general solution (12.6). In order for the solutions (12.16) and (12.18) to match smoothly at the interface, we must have both $w_u = w_l$ and $w_{uz} = w_{lz}$ at $z = 0$. These conditions applied to (12.16) and (12.18) imply that

$$\hat{A} = \hat{C} \quad \text{and} \quad -\mu_u \hat{A} = m_l \hat{B} \tag{12.20}$$

It follows from (12.18) and (12.20) that

$$w_l = \hat{A}\left(-\frac{\mu_u}{m_l}\sin m_l z + \cos m_l z\right) f(x) \tag{12.21}$$

If we consider a location far enough to the lee of the ridge, where the ground is level, then $w_l = 0$ at the ground. If we assign to ground level the height $z = -z_o < 0$, then for w_l to be zero, (12.21) implies that

$$\cot(m_l z_o) = -\frac{\mu_u}{m_l} \tag{12.22}$$

By graphing each side of this equation as a function of k^2, one finds that the graphs cross at one or more points only if the condition

$$\ell_L^2 - \ell_U^2 > \frac{\pi^2}{4z_o^2} \tag{12.23}$$

is satisfied. That is, a horizontal wavelength exists that satisfies the equation only if the depth of the lower layer exceeds a certain threshold before waves can be trapped in it. Furthermore, from the definitions (12.17) and (12.19), it is evident that the right-hand side of (12.22) exists only if

$$\ell_L > k > \ell_U \tag{12.24}$$

Thus, the condition (12.23) can be satisfied only for a wave number in this range, which is consistent with the fact that waves propagate vertically in the lower layer and decay exponentially in the upper layer.

Figure 12.6 shows the flow over the two-dimensional bell-shaped ridge described by (12.14) for a case in which the stratification of the undisturbed flow supports trapped waves. The interface level is at 500 mb (about 5 km altitude). Note that although the profiles of temperature and wind are continuous in z, the value of ℓ^2 is discontinuous, having different constant values above and below the interface. From Fig. 12.6a, it is evident that the trapped waves are indeed confined to the lower layer. It is also apparent that they have no tilt. The latter result is surprising since solutions in the lower layer are of the form of vertically propagating waves, whose phase lines tilt. The explanation lies in the fact that vertically propagating waves cannot continue to propagate upward when they reach the upper layer. Instead they are reflected as downward-propagating waves, which are reflected back up when they reach the ground. As the waves of various wave numbers undergo this multiple reflection process downstream, a superposition of upward- and downward-propagating waves is established. Since the upward- and downward-propagating waves have opposite tilt, their superposition results in no tilt at all. The trapped waves in the figure can be described as having the form

$$w(x,z) = \hat{\beta}\sin\hat{\alpha}z\cos kx \tag{12.25}$$

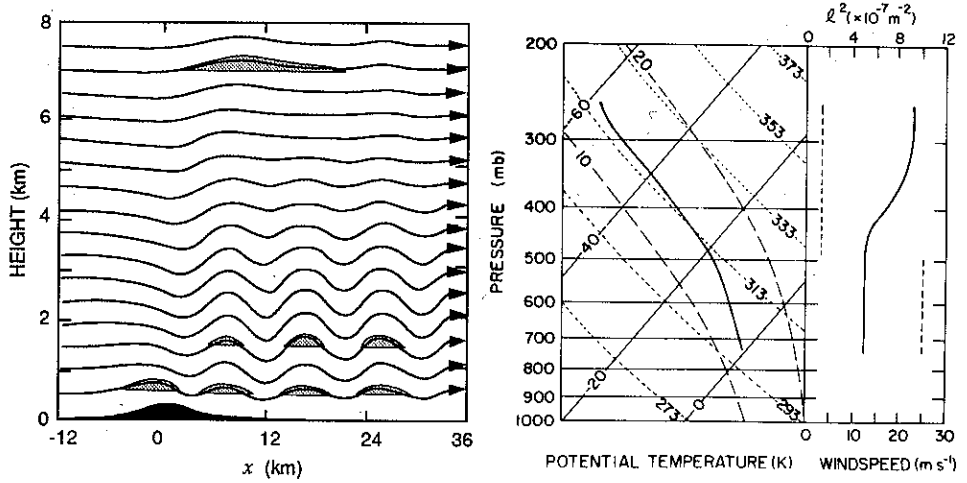

Figure 12.6 (a) Streamlines of steady flow over an isolated two-dimensional bell-shaped ridge for a case in which the stratification of the undisturbed flow supports trapped waves. Lighter shading indicates possible locations of clouds. Darker shading indicates bottom topography. (b) The vertical distribution of temperature and wind speed (solid lines) in the undisturbed flow. This temperature and wind layering implies a discontinuous two-layer structure for the Scorer parameter (dashed line on right panel). (From Durran, 1986b. Reprinted with permission from the American Meteorological Society.)

where $\hat{\beta}$ and $\hat{\alpha}$ are constants. From trigonometric identities, it can be seen that this expression is the sum of equal-amplitude upstream- and downstream-tilting waves

$$w(x,z) = \frac{\hat{\beta}}{2}\sin(\hat{\alpha}z + kx) + \frac{\hat{\beta}}{2}\sin(\hat{\alpha}z - kx) \tag{12.26}$$

Figure 12.6a indicates that the horizontal scale of the trapped lee waves is ~10 km. For typical values of stability and wind, wavelengths are in the range of 5–25 km. Thus, in general, lee waves are of shorter wavelength than the pure vertically propagating waves. Possible locations of clouds are shaded in Fig. 12.6a. The clouds associated with the lee waves are ~3–5 km in horizontal scale. They can often be distinguished from the clouds associated with vertically propagating waves by their repetition downstream of the ridge and by their smaller horizontal scale. In Fig. 12.7, a satellite photograph illustrates an example of numerous lee waves occurring in a regime of strong northwesterly winds aloft over the mountainous western United States.

It is not uncommon for lee wave clouds and clouds associated with a vertically propagating wave to be present in the same situation. Figure 12.6a shows this possibility schematically, where, in addition to the lee-wave clouds downstream of the mountain ridge, a cap cloud is indicated over the crest of the mountain ridge at low levels and a downstream cirrus cloud is indicated aloft. These latter two cloud types are qualitatively similar to those in Fig. 12.4. The weak vertically propagating wave structure appears in addition to the lee waves because the mountain ridge produces some forcing at wave numbers $k < \ell_U$, thus generating waves that can propagate through the upper layer. The larger horizontal scale of the clouds associated with the vertically propagating wave in the upper layer accounts for the greater width of the upper-level cloud compared to the lee-wave clouds below. An actual example of clouds similar to those indicated in Fig. 12.6a is shown in Fig. 12.8. The cap cloud over the crest of the main ridge is seen in the background. Ahead of it are two rows of lee-wave clouds at lower levels, and the wider sheet of cirriform cloud in the foreground aloft is generated by the vertically propagating wave motion.

12.2.5 Nonlinear Effects: Large-Amplitude Waves, Blocking, the Hydraulic Jump, and Rotor Clouds

The preceding analysis relies on linearized equations to describe the dynamics of wave-induced clouds. Under certain atmospheric conditions, nonlinear processes and large-amplitude waves become important in the flow over a mountain ridge. These processes can be studied with nonhydrostatic numerical models—the same type used to study convective clouds (Sec. 7.5.3). Figure 12.9 is an example of the type of model airflow that can develop when large-amplitude waves are present. Shading indicates locations where clouds could appear if layers of air were moist enough. Four types of clouds are indicated, three of which are the same features that appear in the linear case (cf. Fig. 12.6a). The low-level cloud over the crest

Figure 12.7 Visible satellite imagery showing wave clouds over the southwestern United States, 1715 GMT, 2 May 1984.

Figure 12.8 Looking upwind at wave clouds. In the background, lower right, a cap cloud is seen over the Continental Divide, which is the main orographic barrier. The mountains in the foreground, which appear larger in the photo, are actually smaller foothills. In the middle and foreground are two rows of lee-wave clouds induced by the Divide. The cirriform cloud deck at higher levels is produced by the upward air motion associated with a vertically propagating wave. Boulder, Colorado. (Photo by Dale R. Durran.)

and the upper-level cloud just downwind of the ridge are associated with the vertically propagating wave. In this case, the low-level cloud is usually referred to as the *Föhn* wall (Figs. 1.23–1.25). The large-amplitude wave structure is characterized by strong downslope winds (or *Föhn*), and the cloud over the ridge extends just over the crest such that it appears as a wall to an observer on the lee side of the ridge. Lee-wave clouds are again associated with trapped waves downstream of the ridge. These are shown in the shading pattern as the two small clouds

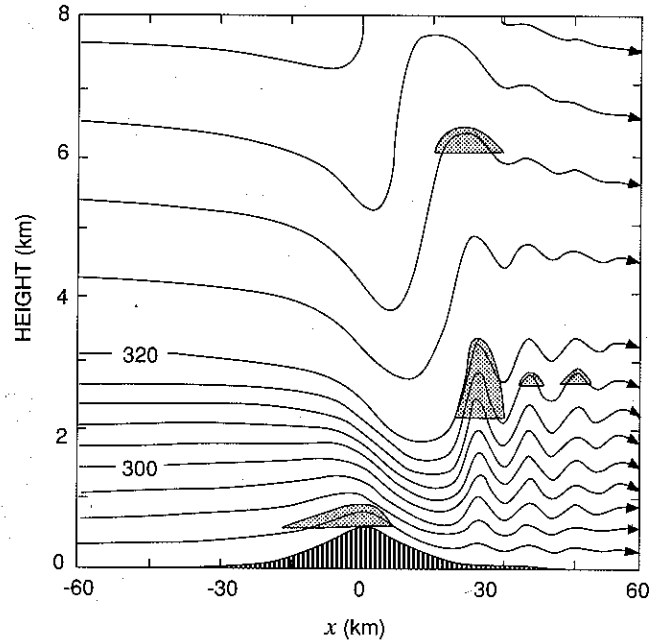

Figure 12.9 Numerical-model results illustrating two-dimensional adiabatic flow that can develop when large-amplitude waves are present. The atmosphere was specified to consist of a less stable layer aloft and a more stable layer below to trap waves in the lower layer. Contours of potential temperature (equivalent to streamlines) are labeled in K. Shading indicates locations where clouds could appear if layers of air were moist enough. (Adapted from Durran, 1986a. Reproduced with permission from the American Meteorological Society.)

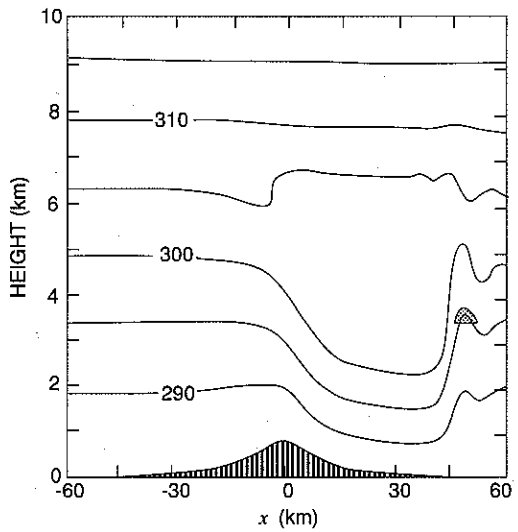

Figure 12.10 Numerical-model results illustrating two-dimensional adiabatic flow that can develop when large-amplitude waves are present. In this case the mean state has a critical layer and wave breaking occurs. Contours of potential temperature (equivalent to streamlines) are labeled in K. Shading indicates location where a cloud could appear if the layer of air were moist enough. (From Durran and Klemp, 1987 as reprinted in Durran, 1990. Reprinted with permission from the American Meteorological Society.)

farthest downwind. The new feature that appears as a result of nonlinear effects, is the rotor cloud. It appears at the sudden vertical jump at the downstream endpoint of the very strong downslope winds, which form immediately to the lee of the ridge and accelerate down the mountain.

Figure 12.10 shows another example of strong downslope winds and possible rotor cloud formation associated with a strong jump in the flow downstream of the ridge. The strong downslope winds, strong upward jump of the air motion, and rotor cloud in these examples are manifestations of large-amplitude wave motion that can occur in three kinds of situations:[324]

1. *Wave breaking*. This case occurs when downstream of the ridge, the θ surfaces overturn, producing a layer of low stability and nearly stagnant flow. This structure, sometimes referred to as a "local critical layer,"[325] is seen at 3.6 km altitude downstream of the mountain in Fig. 12.10. Vertically propagating waves cannot be transmitted through the layer of near-uniform θ centered at about 4 km. The waves excited by the mountain barrier are thus reflected, and wave energy is trapped between this layer and the surface on the lee side of the barrier. If the depth of the cavity between the self-induced critical layer and the mountain slope is suitable, the reflections at the critical layer produce a resonant wave that amplifies in time and produces the strong downslope surface winds and downstream jump.

2. *Capping by a mean-state critical layer*. A local critical layer need not be induced by wave breaking. If the air impinging on the mountain ridge contains a critical layer in its mean-state wind stratification, the necessary reflections, resonance, and amplification may occur on the lee side to produce the downslope winds and downstream jump, even if the mountain is otherwise too small to produce breaking waves. The example in Fig. 12.10 is a case in which both a critical layer is present in the mean state and breaking waves occur.

3. *Scorer parameter layering*. This situation arises when the mountain is too small to force breaking waves but large enough to produce large-amplitude waves in an atmosphere with constant $\bar{u}$ and a two-layer structure in $\bar{B}_z$. Figure 12.9 is an example of this case, in which vertically propagating waves are partially reflected. When the less stable (low $\bar{B}_z$) layer aloft and the more stable (high $\bar{B}_z$) lower-level layer are suitably tuned, superposition of the reflecting waves produces the strong downslope surface winds and downstream jump.

The strong downslope winds and downstream jump, where the rotor cloud occurs, have the characteristics of a special type of flow referred to as a *hydraulic jump*, which occurs in a variety of geophysical situations and is characterized by a sudden change in the depth and velocity of a layer of fluid. For example, a tidal flow up a river is sometimes characterized by such a jump.[326] A hydraulic jump

[324] See Durran (1990).

[325] In general, a *critical layer* is defined as one in which the horizontal phase speed of a gravity wave is equal to the speed of the mean flow.

[326] The river Severn in England is famous for its tidal hydraulic jump, which surfers have been known to ride for several kilometers upstream. See Lighthill (1978) or Simpson (1987).

can also occur downstream of the flow over an obstacle—as in the case of the flow over a rock in a stream, where a turbulent jump in the fluid depth is often seen just downstream of the rock. The latter case is analogous to the atmospheric flow that produces a rotor cloud.

To investigate this type of flow quantitatively, let us consider the steady flow of a homogeneous fluid over an infinitely long ridge. Such a flow is governed by the two-dimensional steady-state shallow-water momentum and continuity equations, which may be written as

$$u\frac{\partial u}{\partial x} = -g\frac{\partial\left(H+\hat{h}\right)}{\partial x} \tag{12.27}$$

and

$$\frac{\partial uH}{\partial x} = 0 \tag{12.28}$$

respectively, where x is perpendicular to the ridge, u is the velocity in the x-direction, H is the vertical thickness of the fluid, and $\hat{h}$ is the height of the obstacle. The pressure gradient acceleration on the right-hand side of (12.27) is equivalent to that on the right-hand side of (2.99), in the case where the term $\delta\rho$ in (2.99) is assumed to be $\approx\rho_1$ (which is the case if the upper layer is air and the lower layer is water).

Flow described by (12.27) and (12.28) may be classified according to the speed of the flow u in relation to $\sqrt{gH}$, which is approximately the phase speed of linear shallow-water gravity waves [$\sqrt{g\bar{h}}$ according to (2.104)]. To make this classification, it is useful to define a *Froude number* (Fr), such that

$$\mathrm{Fr}^2 \equiv \frac{u^2}{gH} \tag{12.29}$$

Then (12.27) may be written as

$$\tfrac{1}{2}u^2 + g\left(H+\hat{h}\right) = \text{constant} > 0 \tag{12.30}$$

or

$$\left(\tfrac{1}{2}\mathrm{Fr}^2+1\right)H = \hat{h}_c - \hat{h} \tag{12.31}$$

where $\hat{h}_c$ is a positive constant. Since the left-hand side must be positive, the condition

$$\hat{h} < \hat{h}_c \tag{12.32}$$

must be satisfied. If $\hat{h} > h_c$, no solution of (12.27) exists and the flow is *blocked*, because it is not energetic enough to surmount the ridge. The smaller the Fr, the more likely the flow will be blocked.

Since (12.27) cannot be solved under blocking conditions, blocked flows must be either nonsteady or three-dimensional. In Sec. 12.3, we will examine three-

dimensional flows at low Froude number around isolated mountain peaks and see that when the flow cannot go over the mountain, it turns laterally and goes around. Here we are concerned with two-dimensional steady-state flows for which (12.27) has solutions (i.e., cases for which (12.32) is satisfied and, hence, the flow can get over a purely two-dimensional barrier). To examine these cases, it is useful to combine (12.27), (12.28), and (12.29) to obtain

$$\left(1-\mathrm{Fr}^{-2}\right)\frac{\partial\left(H+\hat{h}\right)}{\partial x} = \frac{\partial\hat{h}}{\partial x} \tag{12.33}$$

This equation states that the free surface of the fluid can either rise *or fall* as the fluid encounters rising bottom topography. Figure 12.11 indicates various possibilities. In the case of Fr > 1 (Fig. 12.11a), called *supercritical flow*, the fluid thickens and [according to (12.28)] slows down as it approaches the top of the obstacle and reaches its minimum speed at the crest. In the case of Fr < 1 (Fig. 12.11b), called *subcritical flow*, the fluid thins and accelerates as it approaches the top of the obstacle.

Physical insight into supercritical and subcritical flows is obtained by noting that in (12.27) there is a three-way balance among nonlinear advection uu_x, the pressure gradient acceleration associated with the depth of the fluid, and the pressure gradient acceleration induced by the ridge displacing the fluid vertically. The nonlinear advection can be related to the Froude number, since the continuity equation (12.28) implies that

$$\mathrm{Fr}^2 = -\frac{uu_x}{gH_x} \tag{12.34}$$

Thus, Fr^2 is the ratio of the nonlinear advection to the pressure gradient acceleration associated with the variation of fluid depth. Also, the minus sign shows that these two effects are always in opposition.

In the supercritical case (Fr > 1), nonlinear advection dominates the pressure gradient produced by a change in fluid thickness [according to (12.34)], and the height of the ridge must produce horizontal variations in pressure in the same sense as changes associated with fluid depth [according to (12.33)]. Hence, the fluid thickens as it passes over the windward side of the ridge (accumulating potential energy and losing kinetic energy) and thins on the lee side. In the subcritical case (Fr < 1), nonlinear advection is dominated by the effect of the fluid-thickness pressure gradient. The only way for this to occur is for the variation in the height of the ridge to produce horizontal variations in pressure that are in the opposite sense of the changes associated with fluid depth. That is, H_x and $\hat{h}_x$ must be of opposite sign, so that the fluid thins (loses potential energy and gains kinetic energy) as it passes over the windward side of the ridge and thickens on the lee side.

Figure 12.11c shows the flow regime that is characterized by a hydraulic jump on the lee side of the ridge. This case is subcritical on the windward side of the ridge to such a degree that the speed of the flow attains a supercritical value just at

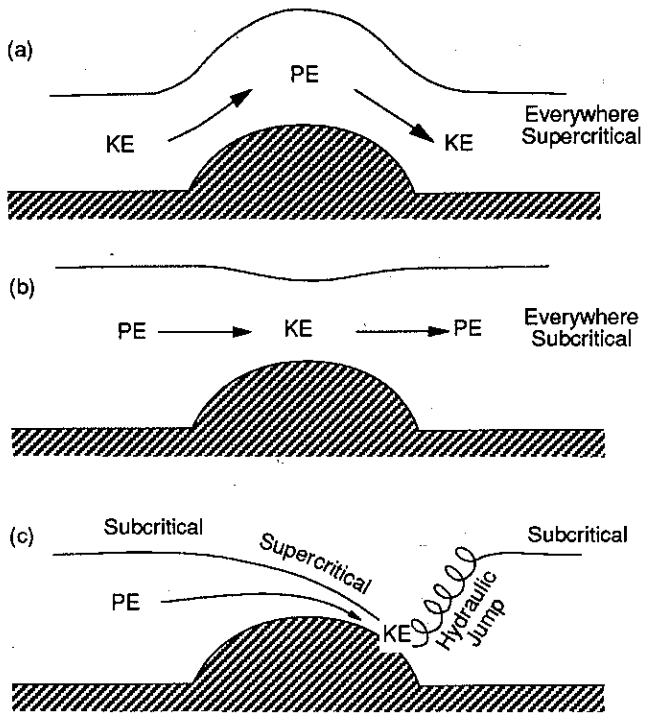

Figure 12.11 Behavior of shallow water flowing over an obstacle: (a) everywhere supercritical flow; (b) everywhere subcritical flow; (c) hydraulic jump. KE and PE refer to kinetic and potential energy, respectively. (Adapted from Durran, 1986a. Reproduced with permission from the American Meteorological Society.)

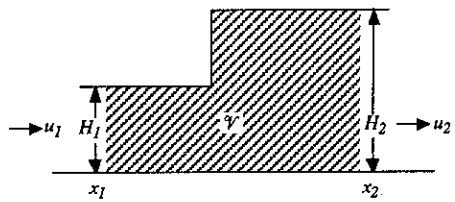

Figure 12.12 A volume of fluid containing a hydraulic jump.

the crest of the barrier. Thus, the flow continues to increase in speed and become still shallower as it runs down the lee slope. In the atmospheric analog to this shallow-water case, severe downslope winds are sometimes a manifestation of the lee-side supercritical flow. Downstream, the strong flow coming down the slope reverts suddenly back to ambient conditions. This sudden transition takes the form of a hydraulic jump.

An important characteristic of the hydraulic jump is that energy is dissipated at the jump. This fact can be inferred by considering a volume of incompressible

fluid $\mathcal{V}$ containing a hydraulic jump, as idealized in Fig. 12.12. The volume $\mathcal{V}$ is bounded by x_1 and x_2 and y and $y + \Delta y$ in a coordinate system that moves with the discontinuity in fluid height. The flow is assumed to be homogeneous (i.e., of constant density) and steady state in this moving coordinate system.

We first consider the mass continuity in the fluid containing the jump by averaging (12.28) to obtain

$$\tilde{Q} \equiv \bar{u}H = \text{constant} \tag{12.35}$$

Next , we consider the conservation of momentum in the mass of fluid contained in $\mathcal{V}$. The equation of motion governing the mean fluid motion is obtained by applying the averaging procedure described in Sec. 2.6 to (2.1), ignoring Coriolis and molecular frictional forces and recalling that the density of an incompressible fluid is constant. The result is

$$\frac{D\bar{\mathbf{v}}}{Dt} = -\nabla\frac{\bar{p}}{\rho} - g\mathbf{k} + \bar{\mathcal{F}} \tag{12.36}$$

Integrating the x-component of (12.36) over the mass of fluid in $\mathcal{V}$ in the moving coordinate system, with substitution from (12.35), and recalling that the pressure at a given level is the weight of the fluid above leads to

$$\tilde{Q}^2 = \frac{g}{2}H_1H_2(H_1 + H_2) + Q_F^2 \tag{12.37}$$

where

$$Q_F^2 = \frac{H_1H_2}{\Delta y(H_1 - H_2)}\iiint_{\mathcal{V}} \mathcal{F}_u \, d\mathcal{V} \tag{12.38}$$

and $\mathcal{F}_u$ is the x-component of $\bar{\mathcal{F}}$. The quantity Q_F^2 in (12.37) can be seen to arise from the drag of turbulence or other small-scale motion. The first term in (12.37) arises from the combination of the horizontal pressure gradient acceleration and the horizontal advection of u.

Now we may examine the energy of the mean flow in the volume $\mathcal{V}$ containing the hydraulic jump. Under the assumed steady-state, two-dimensional conditions, with uniformity in the y-direction, the kinetic energy equation obtained by taking $\bar{\mathbf{v}} \cdot$ (12.36) is

$$\tilde{\mathcal{D}} = \nabla \cdot \left(\frac{\bar{u}^2}{2} + \frac{\bar{w}^2}{2} + gz + \frac{\bar{p}}{\rho}\right)\bar{\mathbf{v}} \tag{12.39}$$

where

$$\tilde{\mathcal{D}} \equiv \bar{\mathbf{v}} \cdot \bar{\mathcal{F}} \tag{12.40}$$

A negative value of $\tilde{\mathcal{D}}$ indicates that energy is being dissipated locally. Integration of (12.39) over the mass of fluid in the volume $\mathcal{V}$ bounded by x_1 and x_2 and y and